Hindawi Publishing Corporation
Journal of Nanomaterials
Volume 2015, Article ID 925268, 9 pages
http://dx.doi.org/10.1155/2015/925268

Research Article

Cd^{2+} Exchange for Na^+ and K^+ in the Interlayer of Montmorillonite: Experiment and Molecular Simulation

Lefu Mei, Huashang Tao, Chao He, Xuebing Xin, Libing Liao, Limei Wu, and Guocheng Lv

Beijing Key Laboratory of Materials Utilization of Nonmetallic Minerals and Solid Wastes, National Laboratory of Mineral Materials, School of Materials Science and Technology, China University of Geosciences, Beijing 100083, China

Correspondence should be addressed to Lefu Mei; mlf@cugb.edu.cn and Libing Liao; clayl@cugb.edu.cn

Received 16 April 2015; Revised 11 June 2015; Accepted 14 June 2015

Academic Editor: Ruomeng Yu

Montmorillonite (Mt) has high cation exchange capacity and thus has been studied extensively for its cation exchange interactions with other cations. However, molecular simulations for the forces governing the cation exchange on Mt surfaces or in the interlayer spaces were limited. In this study, Mt with K^+ and Na^+ in the interlayer spaces was tested for its cation exchange with Cd^{2+} in solution and the forces driving the cation exchange reaction were simulated by molecular simulations. The experimental results showed that Na^+ in Na + Mt was completely exchanged by Cd^{2+}, while only 50% of K^+ in K + Mt was exchanged by Cd^{2+}. A larger *d*-value was noticed for Na + Mt in comparison to K + Mt, suggesting that the interlayer space is more hydrated with Na^+ as the interlayer space cation. Molecular dynamic simulations revealed a larger energy decrease when Cd^{2+} substitutes K^+. However, the nice fit of the K^+ into the 12-coordinated interlayer space sites may restrict its hydration and thus reduce its interlayer space cation exchange capability by Cd^{2+}.

1. Introduction

Cadmium (Cd) has been extensively used in the fields of mining, electroplating, electrolyzing, painting, alloying, plastic generation, and textile processing [1–4]. As Cd is toxic even at very low concentrations, it is classified as a human carcinogen by the US National Toxicology Program. Significant amounts of Cd can be accumulated in food chain and eventually cause health problems in human beings, plants, and animals [1, 2, 5–7]. It is therefore important to develop methods to remove Cd from wastewater before it reaches the natural environments. Various methods developed for the removal and recovery of Cd from industrial wastewater include chemical precipitation, electrolysis, ion exchange, membrane process, and sorption [8–11].

Montmorillonite (Mt) is a 2 : 1 phyllosilicate mineral and has high cation exchange capacity (CEC) that can absorb and retain metal cations in its interlayer space to achieve electrical neutrality. Interlayer space hydrated cations are mainly stabilized by electrostatic interactions, and they could be exchanged by other cations in solution. The species of interlayer space hydrated cations would affect interlayer space, surface area, adsorption, swelling, dispersion, and crystal stability of Mt [12]. The desorption of adsorbed water and interlayer space water in Mt is a one-step or two-step process according to the species of interlayer space cations. The conductivity of Mt is affected by the electrovalence of interlayer space cations much more than by the ionic radius.

Molecular modeling recently has been recognized as an efficient method for understanding the microstructure of interlayer spaces [13–18] in clay minerals. The advantages of molecular modeling include the following: (1) simultaneously present insight into the microstructure of the interlayer spaces at the atomic level and the thermodynamic information of the system [13–16]; (2) conveniently design different models for systematical investigation of the influence of various factors on the characteristics of clay minerals [14, 17, 18]. Numerous studies have employed molecular modeling for understanding the hydration characteristics of clay minerals [13–17]. Hydration energy of K^+-, Na^+-, or Li^+-exchanged Mt was calculated by molecular dynamic (MD) simulations and the results provided thermodynamic explanations for the inhibition of Mt swelling by K^+ [14]. In addition, molecular modeling has also been used to study the adsorption

of contaminants at the interlayer spaces of Mt in several previous reports [19–25]. Moreover, MD simulations can directly predict the adsorption sites for organic contaminants within the interlayer space of organoclays, which include the siloxane surface and the spaces between organic cations [19].

In this study, we investigated cation exchange reaction of Cd^{2+} for K^+ or Na^+ in the interlayer space of Mt experimentally in conjunction with XRD analyses and MD simulation, in order to provide the driving force for interactions between the Mt layers and the interlayer space cation as affected by the cation radii and the degrees of hydration.

2. Materials and Methods

2.1. Materials. The montmorillonite used was SWy-2 obtained from the Clay Mineral Repositories in Purdue University (West Lafayette, IN) and was used without further purification. It has a chemical formula of $(Ca_{0.12}\ Na_{0.32}\ K_{0.05})[Al_{3.01}\ Fe(III)_{0.41}\ Mg_{0.54}][Si_{7.98}\ Al_{0.02}]O_{20}(OH)_4$, a CEC of 85 ± 3 $mmol_c/100\,g$ [26], a layer charge of 0.32 eq/mol per $(Si, Al)_4O_{10}$ [27], an external specific surface area (SSA) of $23\,m^2/g$ [28], and a mean particle size of 3.2 μm with a d_{25} to d_{75} in the range of 3–10 μm.

2.2. Methods. The initial Cd^{2+} concentrations varied from 0.2 to 30 mmol/L for the adsorption isotherm study and were fixed at 2 mmol/L for the kinetic study and pH dependency study. The mass of SWy-2 used was 0.2 g while the volume of solution used was 10 mL for all studies except the kinetic study, in which 20 mL of solution was used. The solid and solution were combined in each 50 mL centrifuge tube and shaken for 2 h at 150 rpm and room temperature for all studies except the kinetic study, in which the shaking time was 1, 3, 5, 30, 60, 120, 600, and 1200 min. After the mixtures were centrifuged at 10000 rpm for 20 min, the supernatants were filtered through 0.22 μm syringe filters before being analyzed for equilibrium Cd^{2+} concentrations.

Free swelling was determined using 1 g of Mt and 100 mL of water in 100 mL graduated cylinder; the mixture was allowed to fully swell with periodic agitation and eventually to set out. The increase of volume after swelling was determined from the difference between the final swelling volume and the initial dry volume of the solid and expressed as mL/g.

Powder XRD analyses were performed on a Rigaku D/max-IIIa diffractometer (Tokyo, Japan) with a Ni-filtered CuKα radiation at 30 kV and 20 mA. Orientated samples were scanned from 4° to 10° at 2°/min with a scanning step of 0.01°. Powder samples were packed in horizontally held trays. The changes in the XRD reflection positions reflect the hydrated size of the metal cations in the interlayer space of Mt.

X-ray fluorescence (XRF) measurements were carried out using a portable XRF spectrometer (Oxford Instruments) with a molybdenum anode, at 25 kV and 0.1 mA. A Si-PIN detector from AMPTEK was employed and characterized by an energy resolution of about 200 eV at 5.9 keV.

FTIR spectra of samples were collected on a Nicolet-560 spectrometer (Thermal Nicolet Co., USA) from 400 to 4000 cm^{-1} with a nominal resolution of 4 cm^{-1}. For each spectrum 16 runs were collected and averaged. The SWy-2 specimens were prepared by adding approximately 1% of the sample powder to dry KBr powder.

Thermogravimetric (TG) analyses were carried out on TGA Q-500 (TA Instruments, New Castle, USA) from room temperature to 800°C, at a heating rate of 10°C/min under a nitrogen flow of 60 mL/min. TG curves were used to determine the percentage of mass loss. Differential scanning calorimetry (DSC) was performed using a differential scanning calorimeter (TA Instruments Q100) fitted with a cooling system using liquid nitrogen. It was calibrated with an indium standard. Samples of 6 mg of Mt were accurately weighed into aluminum pans, sealed, and then heated from 30 to 800°C at 10°C/min under a nitrogen flow of 60 mL/min.

2.3. Computation Details. Molecular simulation was performed under the module "CASTEP" of Materials Studio 6.0 software to investigate the sorption sites of K^+, Na^+, and Cd^{2+} on SWy-2. The primitive unit cell of SWy-2 was optimized with the generalized gradient approximation (GGA) for the exchange-correlation potential (PW91) that is appropriate for the relatively weak interactions present in the models studied. The resulting primitive unit cell was characterized by the parameters a = 15.540 Å, b = 17.940 Å, c = 12.56 Å, and $\alpha = \gamma = 90°$, $\beta = 99°$. Based on the primitive unit cell, a series of (3 × 2 × 1) supercells were built with the d-value of layers set to 10.55, 12.74, and 14.81 Å for K + Mt, Na + Mt, and Cd + Mt, respectively.

3. Results and Discussion

3.1. Preparation of K + Mt. The cation exchangeability of Mt is affected by interaction force of interlayer space cation and Mt layer and force of binding water. To investigate the impact of species of interlayer space cation on cation exchangeability, the experiment was designed first to compare properties of K + Mt and Na + Mt, as Na^+ and K^+ belong to the same main group and have the same electrovalence, but different ionic radii. To keep all conditions the same, except the type of interlayer cations, the Na + Mt was first exchanged with K^+ to prepared K + Mt. After cation exchange by K^+, the Na + Mt was completely converted to K + Mt (Table 1).

The thickness of dehydrated Mt is 9.8 Å, and the interlayer space will be expanded when Na^+ and K^+ hydrated cations enter the interlayer space. As hydration ability of different cations varies, interlayer spaces of Mts with different cations in the interlayer space differ apparently. K^+ concentrations of varying multiples of CEC in solution will result in different amounts of K^+ uptake in Mt, which will result in a change in d_{001} spacing (Figure 1). The d_{001} of original Na + Mt was 12.74 Å. As the amount of K^+ substitution increased, the interlayer space decreased. At an initial input of K^+ at 10 times the CEC of Mt, the d_{001} of Mt reduced to 10.55 Å (Figure 1). However, this d-value is still greater than that of illite or mica, suggesting still presence of limited interlayer space water.

Hydration of cations on interlayer space and outer surface leads to volume expansion of Mt, called free swell. The free swelling of Mt decreased as the amount of K^+ uptake increased (Table 2). Pure Na + Mt had a free swelling of 41.5 mL/g. It decreased to 11.5 mL/g after Na^+ was fully

Table 1: Chemical composition of Mts and their chemical formula.

Chemical composition (%)	Na + Mt	Na + Mt after Cd^{2+} exchange	K + Mt	K + Mt after Cd^{2+} exchange
SiO_2	68.00	62.56	65.38	66.33
Al_2O_3	15.43	14.60	15.16	15.23
Fe_2O_3	5.64	6.75	6.62	6.55
MgO	3.35	2.86	3.51	2.87
CaO	2.36	2.95	3.35	2.12
Na_2O	1.70	0.00	0.24	0.00
K_2O	0.00	0.00	4.73	2.04
CdO	0.00	9.48	0.00	3.66
Chemical formula	$(Na_{0.19}Ca_{0.15})$ $(Al_{1.08}Fe_{0.24}Mg_{0.29})$ $[Si_4O_{10}](OH)_4$	$(Cd_{0.29}Ca_{0.20})$ $(Al_{1.11}Fe_{0.33}Mg_{0.28})$ $[Si_4O_{10}](OH)_4$	$(K_{0.38}Ca_{0.22}Na_{0.03})$ $(Al_{1.11}Fe_{0.31}Mg_{0.33})$ $[Si_4O_{10}](OH)_4$	$(Cd_{0.10}K_{0.16}Ca_{0.14})$ $(Al_{1.12}Fe_{0.31}Mg_{0.26})$ $[Si_4O_{10}](OH)_4$

Table 2: Free swelling (mL/g) of raw Na + Mt and Mt after being in contact with KCl of varying amounts for 120 min.

Na + Mt	0.25 CEC	0.33 CEC	0.5 CEC	0.7 CEC	1 CEC	2 CEC	5 CEC	10 CEC
41.5	36	30	27	21.5	18	14	12	11.5

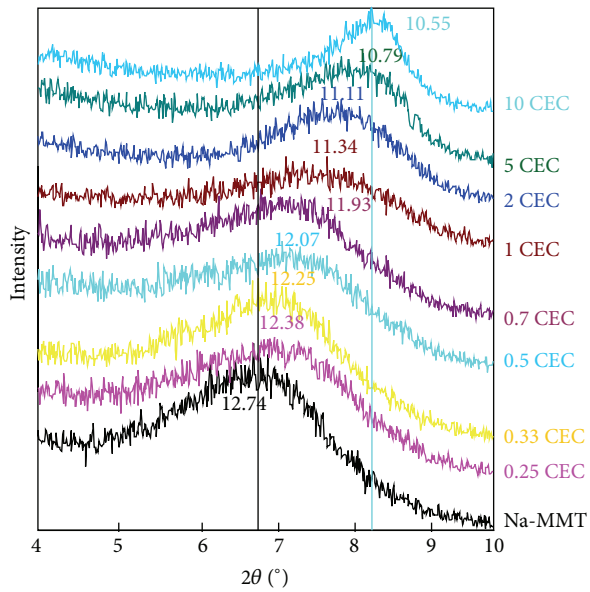

Figure 1: X-ray diffraction patterns of K-MMT. The *d*-spacing is in Å.

replaced by K^+. Generally, a higher free swelling means stronger hydration ability of cations in Mt interlayer space, and better expansion ability means better dispersion after adsorbing water [29]. Different cations have different radii and charges, therefore resulting in different interlayer space stabilities in Mt. As the hydration of Na^+ is obviously stronger than that of K^+, the interlayer space of Na + Mt is greater than that of K + Mt.

3.2. Cd^{2+} Uptake from K + Mt and Na + Mt. Interaction forces between Mt layer and interlayer space cation are electrostatic attraction, intermolecular forces, van der Waals forces, and so forth. Owing to combination of these interactions, metal cations stay stable in the interlayer space place. The experiment used Cd^{2+} to exchange interlayer space cations of Na^+ or K^+ from Na + Mt or K + Mt. By discussing influence of time and concentration of Cd^{2+} on exchanging Na^+ or K^+ from Na + Mt or K + Mt, exchanging rate and volume of two cationic Mts can also be calculated. The difficulty of exchanging cation in Mt interlayer space is relevant with interaction force of interlayer cation and layer, which means stronger interaction force leading to more difficulty in exchange [30].

The cation exchange process of Cd^{2+} for Na^+ or K^+ in the interlayer space of Mt is relatively fast (Figure 2), which can reach 60% of total exchange capacity in 30 min and complete exchange in 2 h, especially for K + Mt, reaching the exchanging balance in 30 min. However, the amount of Cd^{2+} uptake on K^+-Mt was lower than that on Na^+-Mt. The maximal exchange capacity reached 0.43 mmol/g or 0.86 $mmol_c$/g. As the CEC of the original Mt was 0.85 mmol/g, it can be inferred that Na^+ in Na + Mt was completely exchanged while K^+ in K + Mt was only partially exchanged. The Cd^{2+} isotherm data agreed well with the chemical analysis data (Table 1 and Figure 2). This indicated that Mts with different interlayer cations lead to different exchange rate and capacity for Cd^{2+}, which is directly related to the type of interlayer cation [31]. After linear fit of the experimental results, it was found that the exchange Cd^{2+} for Na^+ or K^+ followed the first-order kinetics. The rate constants for Ca^{2+} to exchange K^+ or Na^+ in K + Mt or Na + Mt were 9.8 g/mmol and 3.9 g/mmol, respectively.

The results of XRD analyses indicated the progressive completion of Cd^{2+} exchange for Na in Na + Mt and partial exchange of Cd^{2+} for K^+ in K + Mt. This could be used to determine element composition and content of exchanged Na + Mt and K + Mt and then to calculate the amount of cations exchanged. XRF results showed that the content of Na^+ for Na + Mt after being exchanged by Cd^{2+} is 0 (Table 1), which means interlayer cations are almost all comprised of Cd^{2+} and exchange rate is 100%. On the other hand, more than 40% of the original K^+ was still remaining (Table 1)

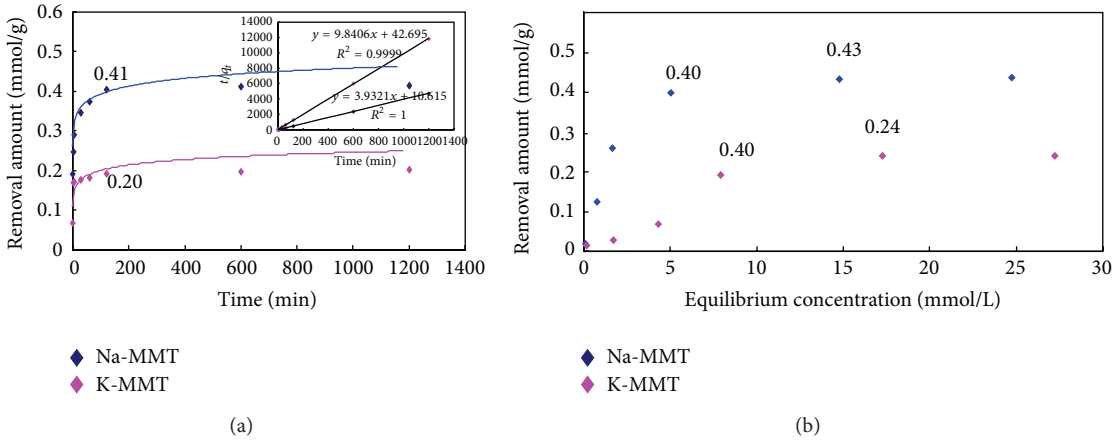

Figure 2: Effect of time/min (a) and Cd^{2+} equilibrium concentration/mmol/L (b) on Cd^{2+} exchanged quantities.

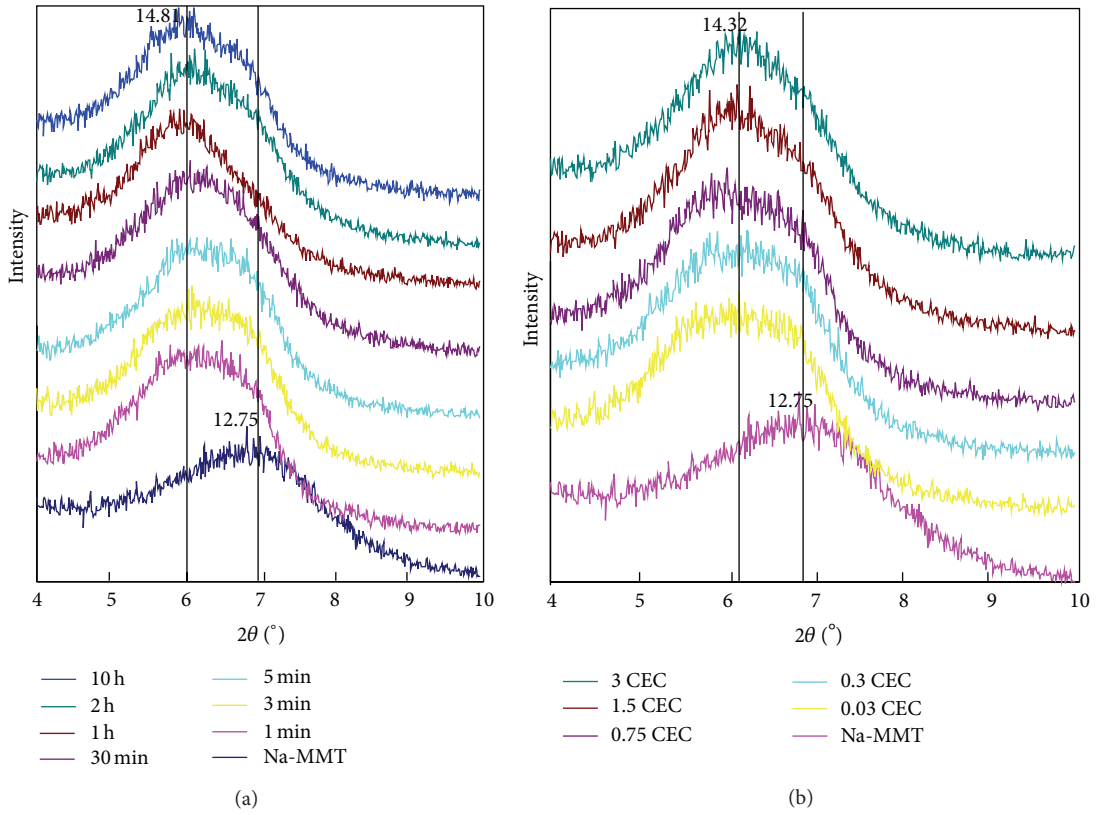

Figure 3: X-ray diffraction patterns of Na-MMT cations exchanged with Cd^{2+} (d in Å). Effect of time/min (a) and Cd^{2+} input in CEC (b).

indicating that K^+ cations were only partially exchanged, even though the input amount of Cd^{2+} was equivalent to 3 times the CEC of the Mt. These results showed that K^+ as the interlayer cation is more stable, as in the case of illite and mica.

The effect of initial solution concentration on exchange capacity had a similar result; that is, the interlayer cation Na^+ in Na + Mt can be completely exchanged by Cd^{2+} ions, the amount of exchange increases as Cd^{2+} concentration increased, and exchange balance was achieved when the input Cd^{2+} was 3 times the CEC. The discrepancy in exchange amounts of Mts with different interlayer space cations is due to diverse interaction forces of layers and interlayer cations [32, 33]. The result of exchange amounts means interaction force between Mt layer and K^+ was greater than that between Mt layer and Na^+. This larger interaction force may prevent complete Cd^{2+} exchange for K^+ in the interlayer space of Mt.

It can be indicated from interlayer space of Mt (Figure 3) that increasing concentration of solution prompts resulted in sharp and enhanced reflection of (001). The d_{001} value of Cd + Mt increased as the amount of Cd^{2+} adsorption increased and reflected at 14.8 Å. This value is larger than 13.15 Å for

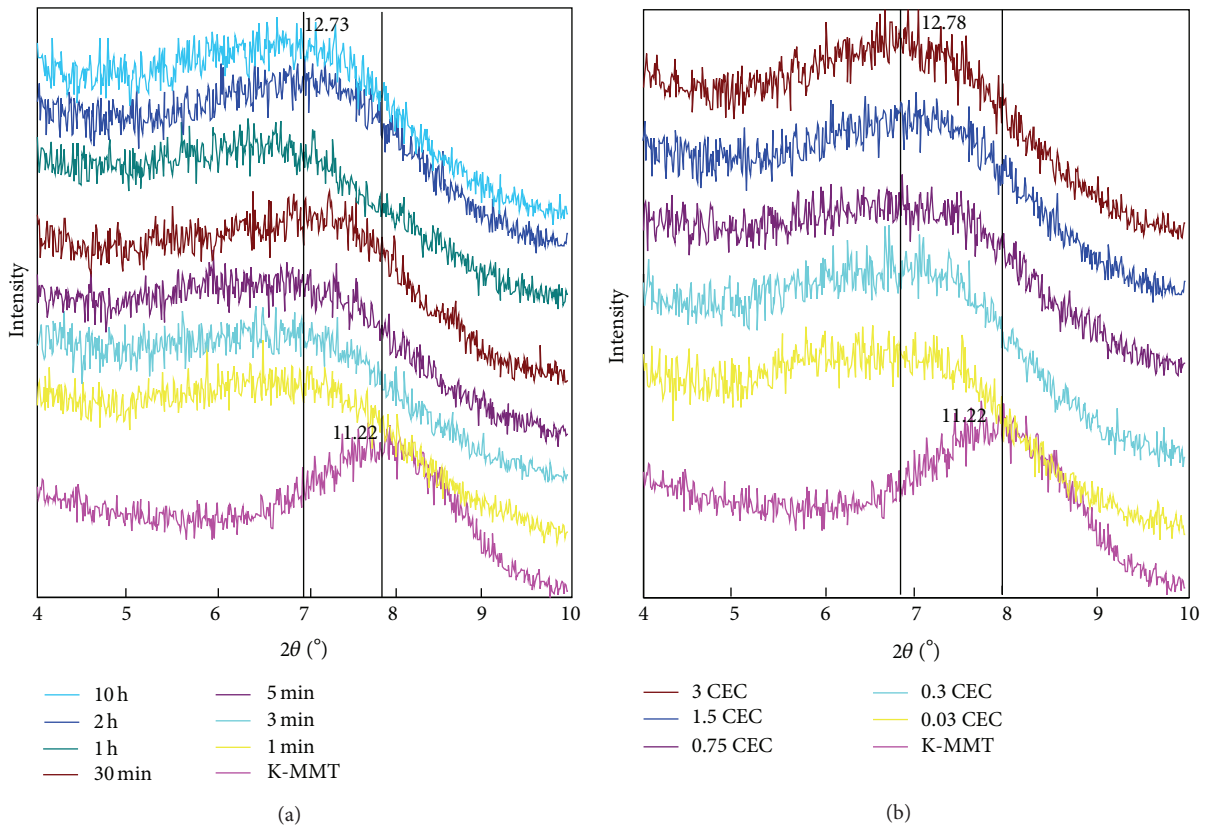

Figure 4: X-ray diffraction patterns of K-MMT cations exchanged with Cd^{2+} (d/Å). Effect of time/min (a) and Cd^{2+} input in CEC (b).

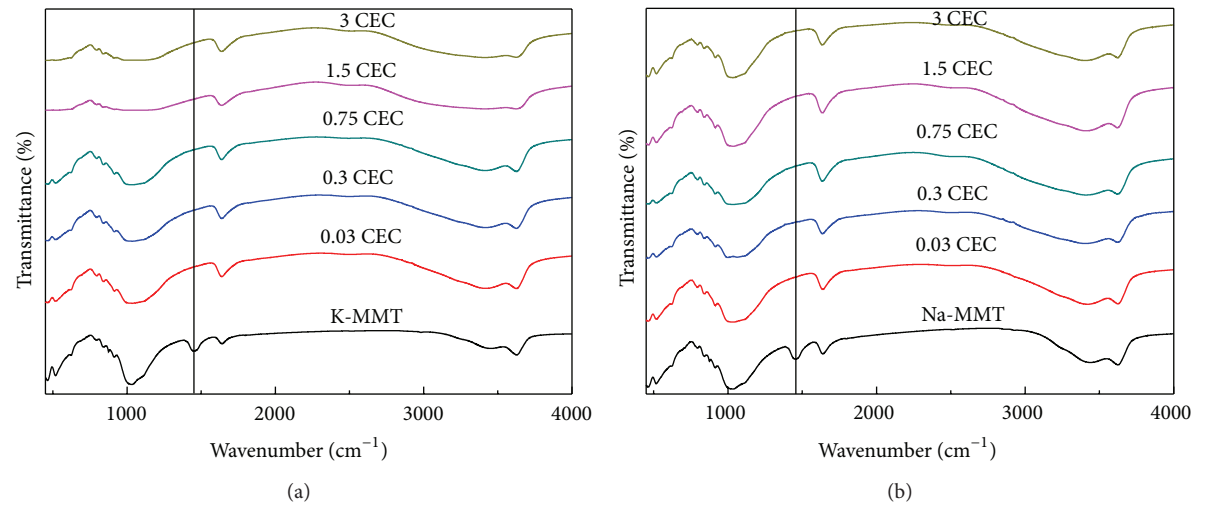

Figure 5: FTIR analyses of K-MMT, Na-MMT, and Cd-MMT.

Pb-exchanged Mt and smaller than 15.90Å for Zn-exchanged Mt [34]. In contrast to Na + Mt, the (001) reflection of K + Mt after being exchanged with different amounts of Cd^{2+} was no longer present, suggesting delamination of Mt (Figure 4).

The FTIR spectra of Mt in contact with different amounts of Cd^{2+} were illustrated in Figure 5. The wide absorbing band observed at 3625 cm^{-1} was assigned to Al-O-H stretching vibration of Mt structural water, and wide adsorbing band at 3436 cm^{-1} could be assigned to stretching of hydroxyl in adsorbed and interlayer space water [35]. The shoulder within 1630~1640 cm^{-1} was due to hydroxyl bending vibration of adsorbed water, while another shoulder observed at about

1035 cm^{-1} could be attributed to stretching of Si-O-Si in Mt lattice. The weak adsorb band observed at 914 cm^{-1} was owing to bending vibration of octahedral hydroxyl in Mt lattice, and the sharp band at 523 cm^{-1} is attributed to bending vibration of Si-O-Al [36].

For K + Mt, as the amount of Cd^{2+} uptake increased, the band within 1630~1640 cm^{-1} increased gradually, while band at 1447 cm^{-1} disappeared. Bands at these two positions are attributed to bending vibration of hydroxyl in adsorbed water, which means changes in interaction force between Mt layer and interlayer cation would lead to variation in position and intensity of these bands. However, the band at 1035 cm^{-1} representing bending vibration of Si-O-Si in Mt lattice and band at 3625 cm^{-1} representing bending of Al-O-H in Mt structural water both decrease as intercalation amount of Cd^{2+} increases, meaning interaction force of K^+ and Mt layer was stronger, leading to a minor change in Mt structure that affected force in layer. For Na + Mt, as Cd^{2+} exchange preceded, except for disappearance of absorption band at 1447 cm^{-1} and increase in transmittance at 1648 cm^{-1}, bands at other positions showed no apparent changes. It means that Na + Mt had a weaker interaction force between the Mt layer and interlayer cations in comparison to K + Mt. This would lead to an easy exchange of Cd^{2+} for Na^+.

The mass change within 25~175°C was due to removal of adsorbed surface and interlayer space water of Mt [37]. For K + Mt, as Cd^{2+} uptake increased, mass loss within 25~175°C increased markedly, from initial 4.1% to 12.9% (Figure 6(a)). The result indicated less amount of interlayer space water in K + Mt in comparison to Cd + Mt, suggesting weaker interaction force between K^+ cation and water molecule than that between Cd^{2+} and water molecules; that is, K^+ was less hydrated than Cd^{2+}. The differential thermal analysis (DTA) curves showed a similar trend within 25~175°C (Figure 6(b)). The endothermic valley was due to removal of interlayer space and adsorbed water. As the amount of Cd^{2+} uptake increased, endothermic valley moves to a slightly higher temperature, indicating that interaction force between Cd^{2+} and water molecule was greater than that between K^+ and water. Mass loss of Na + Mt in 25~175°C was 10.8%, 6.7% more than that of K + Mt (Figure 6(c)), illustrating that Na^+ in Na + Mt was more hydrated than K^+ in K + Mt. As less interlayer space water resulted in smaller interlayer space, a stronger electrostatic attraction of interlayer cation and layers and difficult exchangeability would be anticipated. Therefore, amount of interlayer space water played an important role in easiness of cation exchange for Mt. The mass loss of Na + Mt in 25~175°C increased from initial 10.8% to 17% as the amount of Cd^{2+} uptake increased (Figure 6(c)), while the maximum mass loss after Cd^{2+} exchanging K^+ in K + Mt was only 12.9%. It indicated better cation exchangeability of Na + Mt than K + Mt by Cd^{2+} once again. And in DTA curve (Figure 6(d)), within 25~175°C, endothermic valley remained at the same position as the amount of Cd^{2+} uptake on Na + Mt increased, showing similar interaction force of Na^+ with Cd^{2+} to water molecule, while the amount of combined water of Cd^{2+} was more than Na^+.

3.3. Simulations. Based on the aforementioned experimental results, CASTEP module in Material Studio 6.0 was used to calculate energies of interactions between Mt layers and different cations in the interlayer space. The optimal configuration was speculated when stable cations coexist with Mt layer. The energy of interactions was −78425, −76537, and −75480 eV for Cd^-, Na^-, and K + Mt, respectively, which is positively related to the interlayer space of these three Mts and negatively related to the ionic radii of Cd^{2+}, Na^+, and K^+. Our results agree well with general observations that the smaller the cation, the more hydrated the cation. Apart from that, the interlayer space is also determined by hydration of cation; the more the water molecules surrounded a cation, the greater the interlayer space is [38]. The order of energies in three Mts demonstrates stability of interlayer cations and difficulty in exchange: the higher energy of interactions means better distribution in the interlayer space and more combining water, leading to weaker interaction force with layer, easily exchanged by other cations. Thus, the order of cation exchange preference followed $Cd^{2+} > Na^+ > K^+$.

The interlayer space of K + Mt, Na + Mt, and Cd + Mt was 10.55, 12.5, and 14.81 Å, respectively. MD simulation showed that minimum distances from K^+, Na^+, and Cd^{2+} to oxygen in Mt silicate-oxygen tetrahedron would be 2.303, 2.443, and 4.648 Å, respectively (Figure 7). From top view, it can be seen that K^+, Na^+, and Cd^{2+} are all located on oxygen hexagonal ring, which is above Mg substituting position of alumina in octahedron; maximum angles between the three ions to the nearest oxygen and diagonal oxygen were 102.58°, 103.36°, and 54.28°. From the relations of distance and angle of interlayer cation and oxygen in Mt, silica-oxygen tetrahedron, interaction force of K^+ and Mt layer is the strongest, the distance is less than 2.5 Å, and the angle is obtuse; thus it is possible to form chemical bonds. While interaction force of Na^+ and Mt layer is weaker than that of K^+, so the exchange capacity of Na^+ is higher than that of K^+. The interlayer cations are all hydrated, where minimal distance of K^+, Na^+, or Cd^{2+} to oxygen in water molecular was 2.965, 2.274, or 3.83 Å, respectively. Only Na^+-O distance is less than 2.5 Å, suggesting forming a weak bond.

One Na^+ cation is surrounded by two water molecules, while distances from the central cation to the two water molecules were different. Distances from K^+ or Cd^{2+} to oxygen in water molecules were all longer than 2.5 Å, impossible to form a chemical bond. In addition, the position of Cd^{2+} to water differs from that of Na^+ and K^+, as Na^+ and K^+ are surrounded by two water molecules, monolayer arranged, while Cd^{2+} is surrounded by four water molecules and bilayer arranged. This would lead to expansion of the interlayer space to 14.81 Å. The interaction force of K^+ and Mt layer is the strongest, and that of K^+ and

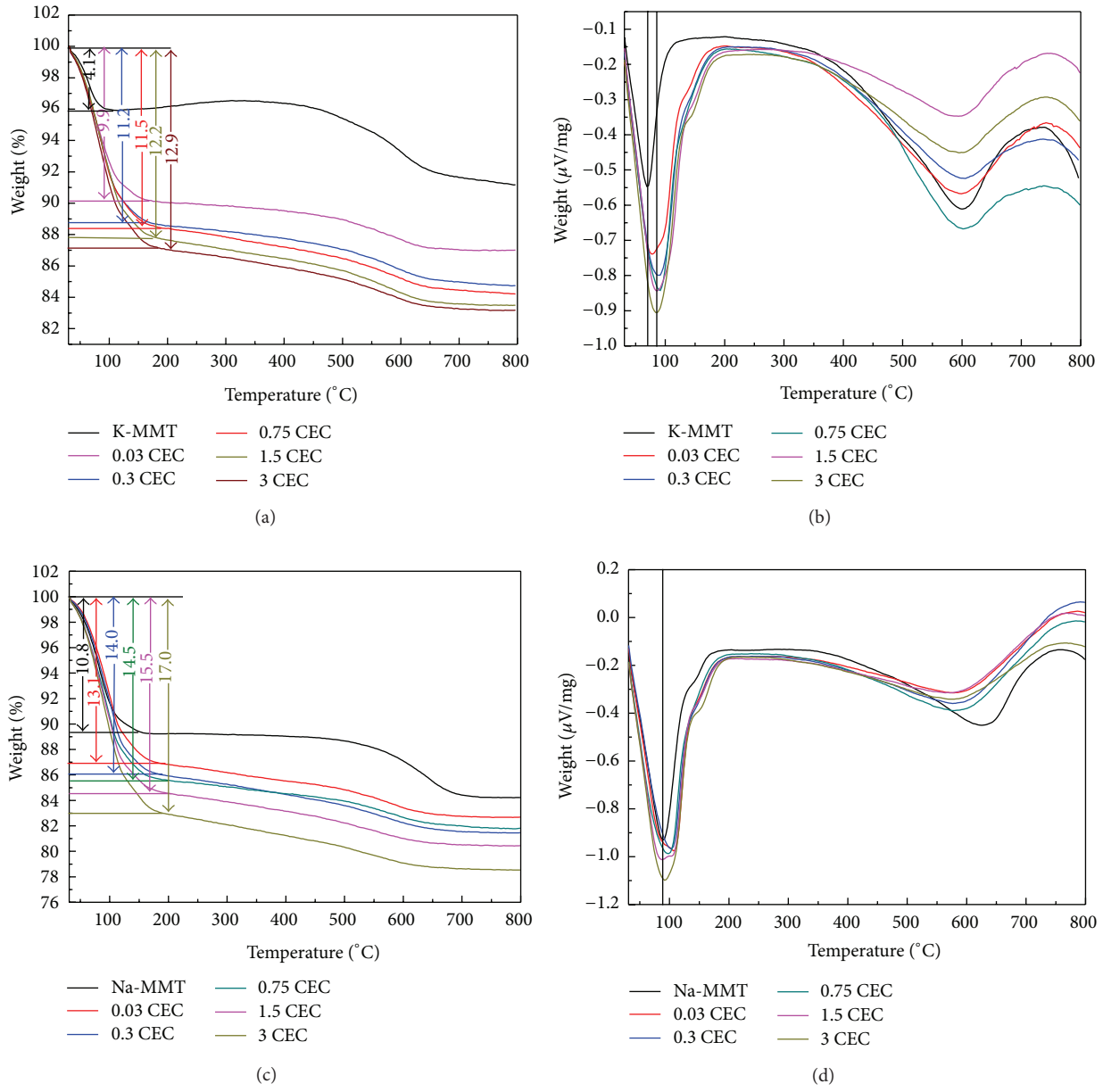

Figure 6: TG and DTA curves of K-MMT (a, b), Na-MMT (c, d), and Cd-MMT.

water molecular is the weakest; interaction force of Na^+ and water is the weakest, resulting in a higher free swelling of Na + Mt.

4. Conclusions

Cd^{2+} was tested to exchange with different interlayer cations in Mts. By comparing exchange capacity, interlayer space, and energy, we discovered great diversity in degrees of cation exchange of different Mts. Na + Mt can be thoroughly exchanged by Cd^{2+}. Conversely, only 60% of K in Mt can be exchanged by Cd^{2+} at an input amount equivalent to 3 times the CEC. The result of XRD indicated that exchange of Na^+ by Cd^{2+} in Mt was uniform and complete, and molecule dynamics simulation proved that electrostatic force of K^+ is larger than that of Na^+, showing an easier cation exchange of Cd^{2+} for Na^+. A better swelling was found for Na + Mt compared to K + Mt, suggesting a better hydration of Na^+ in the interlayer space of Mt. The result of molecule dynamic simulation showed energies of three Mts following Cd + Mt < Na + Mt < K + Mt. Interaction force with Mt layer followed $K^+ > Na^+ > Cd^{2+}$. Therefore, Mts with diverse interaction cations have different properties and should be used in different fields.

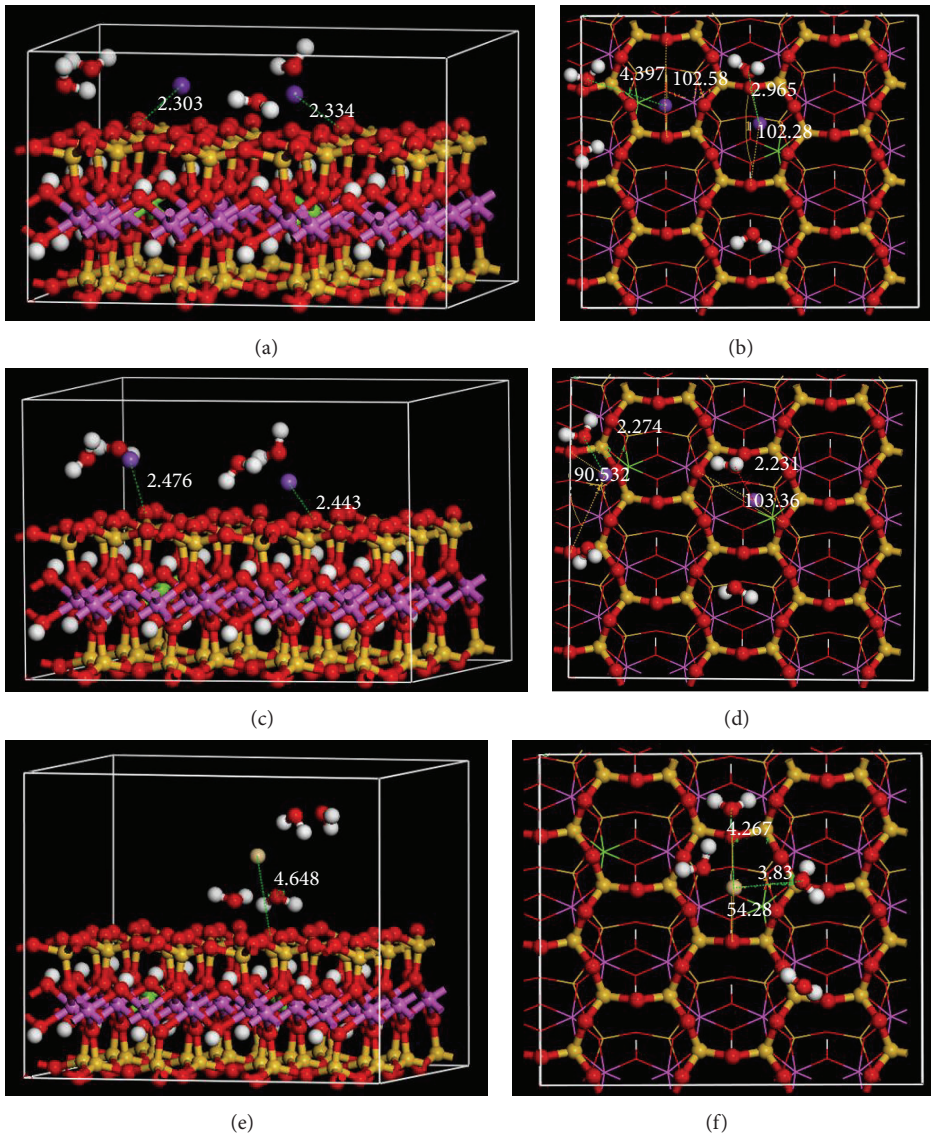

FIGURE 7: Molecular dynamic simulation of the distance and angle of K^+ (a, b), Na^+ (c, d), and Cd^{2+} (e, f) with $[SiO_4]$.

Conflict of Interests

The authors declare that there is no conflict of interests regarding the publication of this paper.

Acknowledgment

This present work was supported by the International S&T Cooperation (Grant no. 2014DFA91000).

References

[1] W. Liu, P. J. Li, X. M. Qi et al., "DNA changes in barley (*Hordeum vulgare*) seedlings induced by cadmium pollution using RAPD analysis," *Chemosphere*, vol. 61, no. 2, pp. 158–167, 2005.

[2] P. F. A. M. Römkens, H. Y. Guo, C. L. Chu, T. S. Liu, C. F. Chiang, and G. F. Koopmans, "Prediction of cadmium uptake by brown rice and derivation of soil-plant transfer models to improve soil protection guidelines," *Environmental Pollution*, vol. 157, no. 8-9, pp. 2435–2444, 2009.

[3] S. Satarug, J. R. Baker, S. Urbenjapol et al., "A global perspective on cadmium pollution and toxicity in non-occupationally exposed population," *Toxicology Letters*, vol. 137, no. 1-2, pp. 65–83, 2003.

[4] E. Dopico, A. R. Linde, and E. Garcia-Vazquez, "Traditional and modern practices of soil fertilization: effects on cadmium pollution of river ecosystems in Spain," *Human Ecology*, vol. 37, no. 2, pp. 235–240, 2009.

[5] Q. Cai, M.-L. Long, M. Zhu, Q.-Z. Zhou, L. Zhang, and J. Liu, "Food chain transfer of cadmium and lead to cattle in a lead-zinc smelter in Guizhou, China," *Environmental Pollution*, vol. 157, no. 11, pp. 3078–3082, 2009.

[6] E. Krznaric, N. Verbruggen, J. H. L. Wevers, R. Carleer, J. Vangronsveld, and J. V. Colpaert, "Cd-tolerant *Suillus luteus*. A fungal insurance for pines exposed to Cd," *Environmental Pollution*, vol. 157, no. 5, pp. 1581–1588, 2009.

[7] M. Vaculík, C. Konlechner, I. Langer et al., "Root anatomy and element distribution vary between two Salix caprea isolates with

different Cd accumulation capacities," *Environmental Pollution*, vol. 163, pp. 117–126, 2012.

[8] M. M. Matlock, B. S. Howerton, K. R. Henke, and D. A. Atwood, "A pyridine-thiol ligand with multiple bonding sites for heavy metal precipitation," *Journal of Hazardous Materials*, vol. 82, no. 1, pp. 55–63, 2001.

[9] I. H. Lee, Y.-C. Kuan, and J.-M. Chern, "Factorial experimental design for recovering heavy metals from sludge with ion-exchange resin," *Journal of Hazardous Materials*, vol. 138, no. 3, pp. 549–559, 2006.

[10] H.-J. Fan and P. R. Anderson, "Copper and cadmium removal by Mn oxide-coated granular activated carbon," *Separation and Purification Technology*, vol. 45, no. 1, pp. 61–67, 2005.

[11] Z. Q. Xie, L. G. Sun, P. F. Zhang et al., "Preliminary geochemical evidence of groundwater contamination in coral islands of Xi-Sha, South China Sea," *Applied Geochemistry*, vol. 20, no. 10, pp. 1848–1856, 2005.

[12] P. Yuan, F. Annabi-Bergaya, Q. Tao et al., "A combined study by XRD, FTIR, TG and HRTEM on the structure of delaminated Fe-intercalated/pillared clay," *Journal of Colloid and Interface Science*, vol. 324, no. 1-2, pp. 142–149, 2008.

[13] V. Marry, B. Rotenberg, and P. Turq, "Structure and dynamics of water at a clay surface from molecular dynamics simulation," *Physical Chemistry Chemical Physics*, vol. 10, no. 32, pp. 4802–4813, 2008.

[14] X.-D. Liu and X.-C. Lu, "A thermodynamic understanding of clay-swelling inhibition by potassium ions," *Angewandte Chemie International Edition*, vol. 45, no. 38, pp. 6300–6303, 2006.

[15] J. Zhou, X. Lu, J. Zhu et al., "Interlayer structure and dynamics of $HDTMA^+$-intercalated rectorite with and without water: a molecular dynamics study," *The Journal of Physical Chemistry C*, vol. 116, no. 24, pp. 13071–13078, 2012.

[16] T. J. Tambach, P. G. Bolhuis, and B. Smit, "A molecular mechanism of hysteresis in clay swelling," *Angewandte Chemie*, vol. 43, no. 20, pp. 2650–2652, 2004.

[17] H. He, J. Galy, and J. F. Gerard, "Molecular simulation of the interlayer structure and the mobility of alkyl chains in $HDTMA^+$/montmorillonite hybrids," *The Journal of Physical Chemistry B*, vol. 109, no. 27, pp. 13301–13306, 2005.

[18] Q. Zhao and S. E. Burns, "Microstructure of single chain quaternary ammonium cations intercalated into montmorillonite: a molecular dynamics study," *Langmuir*, vol. 28, no. 47, pp. 16393–16400, 2012.

[19] R. Zhu, W. Chen, T. V. Shapley, M. Molinari, F. Ge, and S. C. Parker, "Sorptive characteristics of organomontmorillonite toward organic compounds: a combined LFERs and molecular dynamics simulation study," *Environmental Science & Technology*, vol. 45, no. 15, pp. 6504–6510, 2011.

[20] R. Zhu, W. Hu, Z. You, F. Ge, and K. Tian, "Molecular dynamics simulation of TCDD adsorption on organo-montmorillonite," *Journal of Colloid and Interface Science*, vol. 377, no. 1, pp. 328–333, 2012.

[21] J. A. Greathouse and R. T. Cygan, "Water structure and aqueous uranyl(VI) adsorption equilibria onto external surfaces of beidellite, montmorillonite, and pyrophyllite: results from molecular simulations," *Environmental Science and Technology*, vol. 40, no. 12, pp. 3865–3871, 2006.

[22] V. Aggarwal, Y.-Y. Chien, and B. J. Teppen, "Molecular simulations to estimate thermodynamics for adsorption of polar organic solutes to montmorillonite," *European Journal of Soil Science*, vol. 58, no. 4, pp. 945–957, 2007.

[23] M. A. Chappell, D. A. Laird, M. L. Thompson et al., "Influence of smectite hydration and swelling on atrazine sorption behavior," *Environmental Science and Technology*, vol. 39, no. 9, pp. 3150–3156, 2005.

[24] Q. Zhao and S. E. Burns, "Molecular dynamics simulation of secondary sorption behavior of montmorillonite modified by single chain quaternary ammonium cations," *Environmental Science and Technology*, vol. 46, no. 7, pp. 3999–4007, 2012.

[25] P. A. Lock and N. T. Skipper, "Computer simulation of the structure and dynamics of phenol in sodium montmorillonite hydrates," *European Journal of Soil Science*, vol. 58, no. 4, pp. 958–966, 2007.

[26] S. J. Chipera and D. L. Bish, "Baseline studies of the clay minerals society source clays: powder X-ray diffraction analyses," *Clays and Clay Minerals*, vol. 49, no. 5, pp. 398–409, 2001.

[27] D. Borden and R. F. Giese, "Baseline studies of the clay minerals society source clays: cation exchange capacity measurements by the ammonia-electrode method," *Clays and Clay Minerals*, vol. 49, no. 5, pp. 444–445, 2001.

[28] A. R. Mermut and G. Lagaly, "Baseline studies of the clay minerals society source clays: layer-charge determination and characteristics of those minerals containing 2:1 layers," *Clays and Clay Minerals*, vol. 49, no. 5, pp. 393–397, 2001.

[29] N. Khaorapapong and M. Ogawa, "Solid-state intercalation of 8-hydroxyquinoline into Li(I)-, Zn(II)- and Mn(II)-montmorillonites," *Applied Clay Science*, vol. 35, no. 1-2, pp. 31–38, 2007.

[30] L. M. Wu, L. B. Liao, G. C. Lv, F. X. Qin, and Z. H. Li, "Microstructure and process of intercalation of imidazolium ionic liquids into montmorillonite," *Chemical Engineering Journal*, vol. 236, pp. 306–313, 2014.

[31] N. Khaorapapong, A. Ontam, and M. Ogawa, "Formation of ZnS and CdS in the interlayer spaces of montmorillonite," *Applied Clay Science*, vol. 50, no. 1, pp. 19–24, 2010.

[32] A. Meleshyn, "Cetylpyridinium aggregates at the montmorillonite- and muscovite-water interfaces: a Monte Carlo study of surface charge effect," *Langmuir*, vol. 25, no. 11, pp. 6250–6259, 2009.

[33] B. Schampera and S. Dultz, "Determination of diffusive transport in HDPy-montmorillonite by H_2O-D_2O exchange using in situ ATR-FTIR spectroscopy," *Clay Minerals*, vol. 44, no. 2, pp. 249–266, 2009.

[34] W. Oueslati, M. Mefath, H. B. Rhaiem, and A. B. H. Amara, "Cation exchange selectivity versus concentration of competing heavy metal cations (Pb^{2+}, Zn^{2+}): case of Na-montmorillonite," *Physics Procedia*, vol. 2, pp. 1059–1063, 2009.

[35] J. Madejová and P. Komadel, "Baseline studies of the clay minerals society source clays: infrared methods," *Clays and Clay Minerals*, vol. 49, no. 5, pp. 410–432, 2001.

[36] G. C. Lv, L. Liu, Z. H. Li, L. B. Liao, and M. T. Liu, "Probing the interactions between chlorpheniramine and 2:1 phyllosilicates," *Journal of Colloid and Interface Science*, vol. 374, no. 1, pp. 218–225, 2012.

[37] Z. H. Li and W.-T. Jiang, "A thermogravimetric investigation of alkylammonium intercalation into rectorite," *Thermochimica Acta*, vol. 483, no. 1-2, pp. 58–65, 2009.

[38] X. Liu, X. C. Lu, R. C. Wang, H. Q. Zhou, and S. J. Xu, "Molecular dynamics insight into the cointercalation of hexadecyltrimethyl-ammonium and acetate ions into smectites," *The American Mineralogist*, vol. 94, no. 1, pp. 143–150, 2009.